0022-3565/10/3342-449–459$20.00
THE JOURNAL OF PHARMACOLOGY AND EXPERIMENTAL THERAPEUTICS
JPET 334:449–459, 2010

Vol. 334, No. 2
166348/3606923
Printed in U.S.A.

Effect of Dimerized Thrombin Fragment TP508 on Acute Myocardial Ischemia Reperfusion Injury in Hypercholesterolemic Swine

Shizu Oyamada, Robert Osipov, Cesario Bianchi, Michael P. Robich, Jun Feng, Yuhong Liu, Thomas A. Burgess, Timothy M. Bell, Michael R. Sheller, and Frank W. Sellke

Cardiovascular Research Center, Division of Cardiothoracic Surgery, Rhode Island Hospital and Alpert Medical School, Brown University, Providence, Rhode Island (S.O., R.O., C.B., M.P.R., J.F., Y.L., T.A.B., F.W.S.); and Capstone Therapeutics, Tempe, Arizona (T.M.B., M.R.S.)

Received February 1, 2010; accepted May 10, 2010

ABSTRACT

The thrombin-related peptide TP508 is a 23-amino acid monomer that represents a portion of the receptor binding domain in the thrombin molecule. TP508 is also known to readily convert to a dimer in an aqueous environment. In this study the dimeric form of TP508 was investigated in a porcine model of acute myocardial ischemia reperfusion injury (and compared with its monomer). Twenty-four hypercholesterolemic pigs underwent 60 min of mid-left anterior descending coronary artery occlusion followed by 120 min of reperfusion and received either vehicle ($n = 6$), TP508 monomer ($n = 6$), or two different doses of dimer ($n = 6$). Infarct size was significantly reduced in the monomer and two dimer groups compared with vehicle. Improvement in both endothelium-dependent and -independent coronary microvascular relaxations was also observed in treated groups. In addition, the expression of 27-kDa heat shock protein, αB-crystalline, and phosphorylated B-cell lymphoma 2 (Ser70) in the ischemic area at risk were higher in treated groups than in vehicle, whereas the expression of cleaved poly-ADP ribose polymerase was lower in treated groups. Finally, there were fewer apoptotic cells in treated groups than in vehicle. This study suggests that TP508 dimer provides a myocardial-protective effect on acute ischemia reperfusion injury in hypercholesterolemic swine, similar to TP508 monomer, by up-regulating cell survival pathways or down-regulating apoptotic pathways.

The thrombin fragment TP508, also known as rusalatide acetate or Chrysalin, is a 23-amino acid peptide that represents a portion of the highly conserved, catalytic site of the receptor binding domain in the native thrombin molecule. TP508 is known to have an effect on cells and tissues, accelerating dermal wound healing (Carney et al., 1992), fracture repair (Wang et al., 2005), and bone formation (Sheller et al., 2004) and stimulating angiogenesis (Carney et al., 1992; Stiernberg et al., 2000). Previous studies demonstrated that intravenously administered TP508 decreased myocardial necrosis and apoptosis after ischemia reperfusion injury in normocholestrolemic and hypercholesterolemic pigs (Osipov et al., 2009a,b). TP508 is a monomer, and it is known that TP508 dimerizes spontaneously in a saline solution. Because TP508 contains a single cysteine residue, it is capable of forming a dimer chemically via formation of a disulfide bond (M. R. Sheller, personal communication) (Fig. 1). According to an in vitro experiment, the dimerized form of TP508 is

This study was supported by the National Institutes of Health National Heart, Lung, and Blood Institute [Grants RO1HL46716, RO1HL69024, RO1HL85647 (to F.W.S.), T32HL076130] (to R.M.O., M.P.R., and Y.L.); the National Institutes of Health [Grant T32HL0074] (to M.P.R.); Capstone Therapeutics, Tempe, AZ (F.W.S.); and a Irving Bard Memorial Fellowship (to R.M.O. and M.P.R.).

Article, publication date, and citation information can be found at http://jpet.aspetjournals.org.

doi:10.1124/jpet.110.166348.

ABBREVIATIONS: AMI-RI, acute myocardial ischemia–reperfusion injury; LV, left ventricular; LVP, LV pressure; LAD, left anterior descending artery; ABG, arterial blood gas; MAP, mean arterial blood pressure; HR, heart rate; AAR, area at risk; %SS, percentage of segmental shortening; TTC, triphenyl tetrazolium chloride; SNP, sodium nitroprusside; Bcl-2, B-cell lymphoma 2; PARP, poly-ADP ribose polymerase; TUNEL, dUTP nick-end labeling; ANOVA, analysis of variance; U-46619, (*Z*)-7-[(1*S*,4*R*,5*R*,6*S*)-5-[(*E*,3*S*)-3-hydroxyoct-1-enyl]-3-oxabicyclo[2.2.1]heptan-6-yl] hept-5-enoic acid; V, vehicle; D group, lower-dose TP508 dimer; DD group, higher-dose TP508 dimer; M group, monodimer dose; M-1, standard dose TP508 monomer; O1, 30 min after occlusion; O2, 60 min after occlusion; R1, 30 min after reperfusion; R2, 60 min after reperfusion; R3, 90 min after reperfusion; R4, 120 min after reperfusion; PAR, protease-activated receptor; HSP, heat shock protein; VT, ventricular tachycardia; VF, ventricular fibrillation; HPLC, high-pressure liquid chromatography.

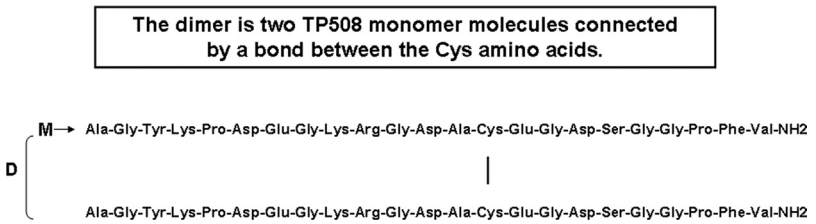

Fig. 1. The sequences of TP508 monomer (M) and dimer (D).

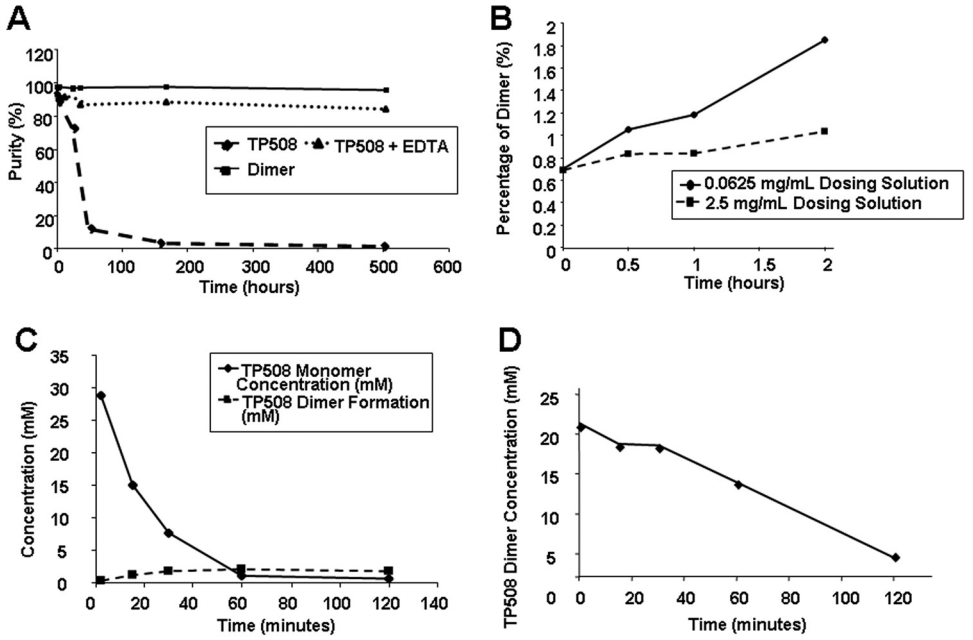

Fig. 2. In vitro analysis of TP508 monomer and dimer. A, a long time solution stability of TP508 monomer and dimer in saline. Shown is a comparison of TP508 monomer and dimer solution stability, providing purity (%) versus time (hours) with TP508 monomer, TP508 monomer + 10 μM EDTA, and TP508 dimer in 0.625 mg/ml sterile saline. The result is at room temperature (~24°C). Ultraviolet HPLC was used for analysis. The purity value used is determined by HPLC percentage area using UV detection and the following formula. The main peak area is the peak area as integrated by the HPLC software for the analyte of interest, such as TP508 monomer or TP508 dimer. The total area is the area of the analyte and all other impurities or degradation products. The purity goes down in value as degradation peaks appear or grow in size. B, TP508 dimer formation in dosing solution. TP508 monomer was prepared at two concentrations in sterile saline (0.0625 and 2.5 mg/ml). These concentrations were selected because they were the lowest and highest infusion concentrations used experimentally. Over the course of 120 min, dimer formation was observed to increase from a starting value of ~0.7 to 1.9% and 1% in the low and high concentration samples, respectively. This demonstrates that dimer formation in the dosing solution was likely to be minimal throughout the infusion period. C, TP508 monomer and dimer concentration in pig plasma versus time. TP508 monomer was added to pig plasma in vitro at a concentration of 70 μg/ml (30.6 mM). The plasma was maintained at 37°C for 120 min. Rapid degradation of TP508 monomer into smaller peptide fragments was observed, with only ~2% of the initial monomer concentration remaining after 120 min. Dimer was observed to form from the TP508 monomer; however, peak dimer concentration reached only 14%. This indicates that although dimer is formed it reaches a maximal concentration that is a fraction of the initial monomer concentration. Accounting for total peptide recovery, which included TP508 monomer, TP508 dimer, and all peptide fragments resulting from enzymatic degradation demonstrated that more than half the monomer was degraded in the first 15 min. Total recovery dropped over time, indicating that some peptide fragments were degraded to the point that they were no longer captured by the HPLC assay or they were bound to plasma proteins. D, TP508 dimer concentration in pig plasma versus time. TP508 dimer was added to pig plasma at a concentration of 26.6 mmol. The plasma was maintained at 37°C for 120 min. Dimer concentration was observed to drop over time, however, less rapidly than was seen for TP508 monomer. Monomer was not detected. This may indicate that the dimer is also degraded in pig plasma; however, it is not reduced to the monomer.

much more stable than monomer in saline (M. R. Sheller, personal communication) (Fig. 2A). Thus, we first performed in vitro experiments to examine the stability of TP508 monomer and dimer in pig plasma over the course of 120 min, which is the length of infusion in the protocol. Second, we performed in vivo experiments to assess the effect of two doses of TP508 dimer in the setting of acute myocardial ischemia–reperfusion injury (AMI-RI) in a swine model compared with standard doses of TP508 monomer. Because a majority of patients presenting with AMI have endothelial dysfunction secondary to dyslipidemia, diabetes, and hypertension, we elected to use hypercholesterolemic swine as a model of endothelial dysfunction in assessing the effect of TP508.

Materials and Methods

Stability of TP508 Monomer and Dimer (In Vitro). First, we assessed the dosing solution stability of TP508 monomer. TP508 monomer was prepared at two concentrations in sterile saline (0.0625 and 2.5 mg/ml). These concentrations were selected because they were the lowest and highest infusion concentrations used in the in vivo experiments described below. The solutions were incubated at room temperature in plastic syringes and analyzed by high-pressure liquid chromatography (HPLC) to determine the extent of dimer formation. Each dosing solution was diluted to 0.200 mg/ml with 0.1% trifluoroacetic acid and analyzed by HPLC.

Next, we assessed the plasma stability of TP508 monomer and dimer. First, TP508 monomer was added to pig plasma (Bioreclamation, Inc., Liverpool, NY) at a concentration of 70 μg/ml (30.6 mM).

This concentration was selected because it represented the highest concentration expected after the bolus dose was complete (60-mg bolus dose into a 20-kg pig with ~850 ml of circulating plasma volume). Degradation of TP508 monomer into smaller peptide fragments was observed over the course of 120 min. Second, TP508 dimer was added to pig plasma (Bioreclamation, Inc.) at a concentration of 26.6 mM. Monomer and dimer concentrations were measured over the course of 120 min. Each plasma sample was maintained at 37°C for 120 min, precipitated with an equal volume of 20% trichloroacetic acid, vortexed for 20 s, and then centrifuged with a microcentrifuge for 10 min at 14,000 rpm. The supernatant was analyzed by HPLC. In vitro experiments were performed at Capstone Therapeutics Research Operations (Tempe, AZ).

Experimental Design (In Vivo). Animals were housed individually and provided with laboratory chow and water ad libitum. All experiments were approved by the Beth Israel Deaconess Medical Center Institutional Animal Care and Use Committee (Boston, MA) and the Harvard Medical Area Standing Committee on Animals (Boston, MA). The experiments conformed to the National Institutes of Health *Guidelines Regulating the Care and Use of Laboratory Animals* (National Institutes of Health publication 5377-3, 1996).

Twenty-four intact (noncastrated) male Yucatan mini-swine (20–22 weeks old) were fed a high-fat/high-cholesterol diet for 4 to 6 weeks (Sinclair Research Center, Columbia, MO) (Spurlock and Gabler, 2008). All animals were subjected to regional left ventricular (LV) ischemia by left anterior descending (LAD) arterial occlusion distal to the second diagonal branch for 60 min. Animals received intravenously either vehicle (V; $n = 6$) or TP508 monomer (M-1; $n = 6$) as a bolus of 0.5 mg/kg (0.21μmol/kg) 50 min into ischemia followed by a continuous infusion of 1.25 mg (0.54 μmol/kg/h) during the entire period of reperfusion, or equivalent dose of TP508 dimer to M-1 expressed in mole (DD; $n = 6$) or half-dose of TP508 dimer as DD (D; $n = 6$) (Harvard Apparatus Inc., Holliston, MA) (Table 1). To assess the dose-dependent effect of TP508 monomer, 12 pigs were added, divided into two groups, and received 1/10 times M-1 (M-1/10; $n = 6$) or four times M-1 (M-4; $n = 6$).

Arterial blood gas (ABG), arterial blood pressure, hematocrit, LV pressure, heart rate (HR), electrocardiography, O_2 saturation, and core body temperature were measured and recorded. Myocardial segmental shortening in the long axis (parallel to the LAD) and short axis (perpendicular to the LAD) were recorded at baseline before the onset of the ischemia and harvest. At the completion of the protocol, the heart was excised, and tissue samples from the ischemic and nonischemic left ventricles were collected for analysis as described below. Thus, each pig served as its own control with regard to molecular studies.

Surgical Protocol. Swine were sedated with ketamine hydrochloride (20 mg/kg i.m.; Abbott Laboratories, Abbott Park, IL) and anesthetized with a bolus infusion of thiopental sodium (Baxter, McGaw Park, IL; 5.0–7.0 mg/kg i.v.), followed by endotracheal intubation. Ventilation with a volume-cycled ventilator (model Narkomed II-A; North American Drager, Telford, PA; oxygen, 40%; tidal volume, 12.5 ml/kg; ventilation rate, 9–11 breaths/min; positive end-expiratory pressure, 3 cm of H_2O; inspiratory to expiratory time, 1:2) was used. General endotracheal anesthesia was established with 3.0% isoflurane (Ultane; Abbott Laboratories) at the beginning of the surgical preparation and maintained with 1.0% isoflurane throughout the experiment. One liter of lactated Ringer intravenous fluid was administered after the induction of anesthesia and continued throughout the surgical protocol at 150 ml/h. Right groin dissection was performed, and the femoral vein and common femoral artery were isolated and cannulated by using six French sheaths (Cordis Corporation, Miami, FL). The right femoral vein was cannulated for intravenous access, and the right common femoral artery was cannulated for arterial blood sampling and continuous intra-arterial blood pressure monitoring (Millar Instruments Inc., Houston, TX). A median sternotomy was performed. A catheter-tipped manometer (Millar Instruments) was introduced through the apex of the heart to record LV pressure. Segmental shortening in the area at risk (AAR) was assessed by using a Sonometric digital ultrasonic crystal measurement system (Sonometrics Corp., London, ON, Canada) using four 2-mm digital ultrasonic probes implanted in the subepicardial layer approximately 10 mm apart within the ischemic LV area. Cardiosoft software (Sonometrics Corp.) was used for data recording (LV dP/dt, segmental shortening, arterial blood pressure, and heart rate) and subsequent data analysis to determine myocardial function. Baseline hemodynamic, functional measurement, ABG analysis, and hematocrit were obtained. ABG analysis was performed at the baseline, 30 min after occlusion, and 30 min after reperfusion. All animals received a bolus of lidocaine (1.5 mg/kg) as prophylaxis against ventricular dysrhythmia and 80 units/kg of intravenous heparin bolus before occlusion of the LAD. The LAD coronary artery was occluded 3 mm distal to the origin of the second diagonal branch with a Rommel tourniquet. Myocardial ischemia was confirmed visually by regional cyanosis of the myocardial surface. The Rommel tourniquet was released 60 min after the onset of acute ischemia, and the myocardium was reperfused for 120 min. At the end of the reperfusion period, hemodynamic and functional measurements were recorded as described above, followed by religation of the LAD and injection of monastryl blue pigment (England Corp., Louisville, KY) at a 1:150 dilution in phosphate-buffered saline into the aortic root after placement of an aortic cross-clamp distal to the coronary arterial ostia to demarcate the AAR. The heart was rapidly excised just after a 50-ml injection of blue pigment, and the entire LV, including the septum, was dissected free. The LV was cut into approximately 1-cm-thick slices perpendicular to the axis of the LAD from the LV apex to the point of ligation, which resulted in four slices. The AAR was clearly identified by the lack of blue pigment staining. The AAR of the second slice proximal to the LV apex was isolated and divided for use in Western blotting and paraffin section. The other three slices were used for infarct size measurement as described below. Ventricular dysrhythmia (ventricular fibrillation or pulseless ventricular tachycardia) events were recorded and treated with immediate electrical cardioversion (100–150 J, internal paddles).

Measurement of Global and Regional Function. Global myocardial function was assessed by calculating the maximal positive first derivative of LV pressure over time (+dP/dt). Regional myocardial function was determined by using subepicardial 2-mm ultrasonic probes to calculate the percentage of segment shortening (%SS), which was normalized to the baseline. Measurements were taken during a period of at least three cardiac cycles in normal sinus rhythm and then averaged. Digital data were inspected for the correct identification of end-diastole and end-systole. End-diastolic segment length was measured at the onset of the positive dP/dt, and the end-systolic segment length was measured at the peak negative dP/dt. Measurements were taken at baseline (Pre) and then every 30 min [30 min after occlusion (O1), 60 min after occlusion (O2), 30 min after reperfusion (R1), 60 min after reperfusion (R2), 90 min after reperfusion (R3), and 120 min after reperfusion (R4)] throughout the protocol using a Sonometrics system as described previously (Osipov et al., 2009a,b).

TABLE 1
List of the dosages used in the surgical protocol
Molecular weight: monomer = 2311.49; dimer = 4621.0.

Group	Drug	Bolus	Infusion
		μmol/kg (mg/kg)	*μmol/kg/h (mg/kg/h)*
M-1	Monomer	0.21 (0.5)	0.54 (1.25)
M-1/10	Monomer	0.021 (0.05)	0.054 (0.125)
M-2*	Monomer	0.43 (1.0)	3.1 (2.5)
M-4	Monomer	0.86 (2.0)	6.2 (5.0)
D	Dimer	0.11 (0.5)	0.27 (1.25)
DD	Dimer	0.21 (1.0)	0.54 (2.5)

*M-2 is not presented in the method of the present study (M-2 is part of an already published group) (Osipov et al., 2009b).

Quantification of Myocardial Infarct Size. Three LV slices were immediately immersed in 1% triphenyl tetrazolium chloride (TTC; Sigma-Aldrich, St. Louis, MO) in phosphate buffer (pH 7.4) at 38°C for 30 min. The infarct area (characterized by the absence of staining), the noninfarcted AAR (characterized by red tissue staining), and the nonischemic portion of the LV (characterized by purple tissue staining) were sharply dissected from one another. The percentage of the AAR was defined as: (infarct mass + noninfarct AAR mass)/total LV mass × 100. Infarct size was calculated as a percentage of AAR to normalize for any variation in AAR size by using the following equation: (infarct mass/total mass AAR) × 100.

Coronary Microvascular Reactivity Studies. Coronary microvascular reactivity was examined in the ischemic territory, as described previously (Osipov et al., 2009a,b). In brief, coronary arterioles were dissected with a 40× microscope. Microvessels were mounted on dual-glass micropipettes and examined in a pressurized, isolated microvessel chamber. ADP (1 nM–100 μM), substance P (0.1 pM–10 nM), and sodium nitroprusside (SNP; 1 nM–100 μM) were applied extraluminally after precontraction by 25 to 50% of the baseline diameter with the thromboxane A2 analog U-46619 [(*Z*)-7-[(1*S*,4*R*,5*R*,6*S*)-5-[(*E*,3*S*)-3-hydroxyoct-1-enyl]-3-oxabicyclo[2.2.1]heptan-6-yl]hept-5-enoic acid] (0.1–1 μM).

Western Blotting. Whole-cell lysate were made from homogenized AAR myocardial samples with RIPA buffer (Boston Bioproduct, Worcester, MA) and centrifuged at 12,000*g* for 10 min at 4°C to separate soluble from insoluble fractions. In the myocardial tissue lysate, the protein concentration was measured spectrophotometrically at 595 nm with a DC protein assay kit (Bio-Rad Laboratories, Hercules, CA). Twenty to 60 mg of total protein was fractionated by 4 to 20%, 8 to 16%, or 12% gradient SDS/polyacrylamide gel electrophoresis (Invitrogen, Carlsbad, CA) and transferred to polyvinylidene difluoride membranes (Millipore Corporation, Billerica, MA). Each membrane was incubated overnight at 4°C with the following antibodies: total and phosphorylated B-cell lymphoma 2 (Bcl-2) (1:200 dilution; Cell Signaling Technology, Danvers, MA), total and cleaved caspase-3 (1:300 dilution; Cell Signaling Technology), total and cleaved poly-ADP ribose polymerase (PARP) (1:300 dilution; Cell Signaling Technology), 27-kDa heat shock protein (HSP) (1:1000 dilution; Assay Designs, Ann Arbor, MI), and αB-crystallin (1:1000 dilution; Assay Designs). The membranes were subsequently incubated for 45 min in diluted secondary antibody (1:2000 dilution; Cell Signaling Technology). Immune complexes were visualized with the enhanced chemiluminescence detection system (GE Healthcare, Little Chalfont, Buckinghamshire, UK). Bands were quantified by densitometry of radioautograph films. Ponceau S staining was performed to confirm equivalent protein loading.

dUTP Nick-End Labeling Staining. The apoptotic cells were identified by dUTP nick-end labeling (TUNEL) using an apoptosis detection kit according to the manufacturer's protocol (Millipore Corporation). At least 1 cm^2 of tissue from the AAR was analyzed from each animal (four per group). The nuclei were viewed and manually counted by an observer blinded to the experimental conditions. The number of TUNEL-positive cardiomyocytes, indicating apoptosis, was divided by the surface area and expressed in the number per 100 mm^2.

Statistical Methods. Functional and microvascular reactivity data were analyzed by two-way repeated-measures ANOVA. Frequency of VT/VF was analyzed by the χ^2 test. Infarct size and densitometry in Western blot data were analyzed by one-way ANOVA. All results were expressed as mean ± S.E.M., and a p value of less than 0.05 was considered statistically significant (Systat Software, Inc., San Jose, CA). Immunoblots were expressed as a ratio of protein to loading band density and analyzed after digitization and quantification of X-ray films with ImageJ 1.33 (National Institutes of Health, Bethesda, MD).

Results

Dosing Solution Stability of TP508 Monomer (In Vitro). Over the course of 120 min, TP508 dimer was observed to increase from a starting value of ~0.7 to 1.9% and 1% in the low and high concentration samples, respectively (Fig. 2B). This demonstrates that TP508 monomer dimerizes in a saline solution over time; however, dimer formation in the dosing solution of the present study is likely to be minimal throughout the 120-min infusion period.

Plasma Stability of TP508 Monomer and Dimer (In Vitro). As shown in Fig. 2C, TP508 monomer rapidly degraded into smaller peptide fragments, with only ~2% of the initial monomer concentration remaining after 120 min. TP508 dimer was observed to form from the TP508 monomer; however, the peak concentration of the dimer reached only ~2.15 mM at 60 min. If 100% of the monomer was converted to dimer, the concentration of dimer would be expected to reach 15.3 mM. Therefore, the conversion of TP508 monomer to dimer in plasma was approximately 14%, suggesting that, although dimer is formed, it reaches a maximum concentration that is a small fraction of the initial monomer concentration. Examination of total peptide recovery, which included TP508 monomer, TP508 dimer, and all peptide fragments resulting from enzymatic degradation, demonstrated that more than half the monomer was degraded in the first 15 min. Total recovery dropped over time, indicating that some peptide fragments were degraded to the point that they were no longer captured by the HPLC assay or they were bound to plasma proteins. As shown in Fig. 2D, dimer concentration was observed to decrease over time, however, less rapidly than was seen for TP508 monomer. Monomer was not detected. The dimer concentration was observed to decrease more slowly over time compared with TP508 monomer. This may indicate that the dimer is also degraded in plasma; however, it is not reduced to the monomer. Although dimer concentration dropped less than was seen for monomer, the total recovery of dimer and degradation products was observed to drop more than for monomer. This may suggest that some dimer loss was caused by precipitation or binding to plasma proteins rather than enzymatic degradation.

Arterial Blood Gas, Hematocrit, Core Temperature. No significant differences were observed among groups in arterial pH, pCO_2, pO_2, hematocrit, and core temperature at any time point in the protocol.

Serum Lipid Profile and Glucose. Levels (mg/dl) of serum total cholesterol (V, 373 ± 67; M-1, 512 ± 15; D, 411 ± 63; DD, 511 ± 63; $p = 0.33$), triglyceride (V, 12 ± 1; M-1, 15 ± 3; D, 12 ± 2; DD, 19 ± 5; $p = 0.76$), HDL (V, 89 ± 13; M-1, 67 ± 9; D, 73 ± 9; DD, 92 ± 13; $p = 0.34$), LDL (V, 281 ± 56; M-1, 443 ± 19; D, 335 ± 57; DD, 415 ± 55; $p = 0.09$), and blood glucose (V, 54 ± 4; M-1, 55 ± 2; D, 59 ± 4; DD, 62 ± 5; $p = 0.47$) at the baseline were not significantly different among groups (Chemistry Laboratory, Rhode Island Hospital).

Global and Regional Left Ventricular Function. Figure 3 shows mean arterial blood pressure (MAP), developed LV pressure (LVP), HR, and global systolic LV function as determined from LV dP/dt from the baseline (pre) to the end of reperfusion (R4). No significant differences were seen among groups between the baseline (pre) and the end of reperfusion (R4) in MAP (p =

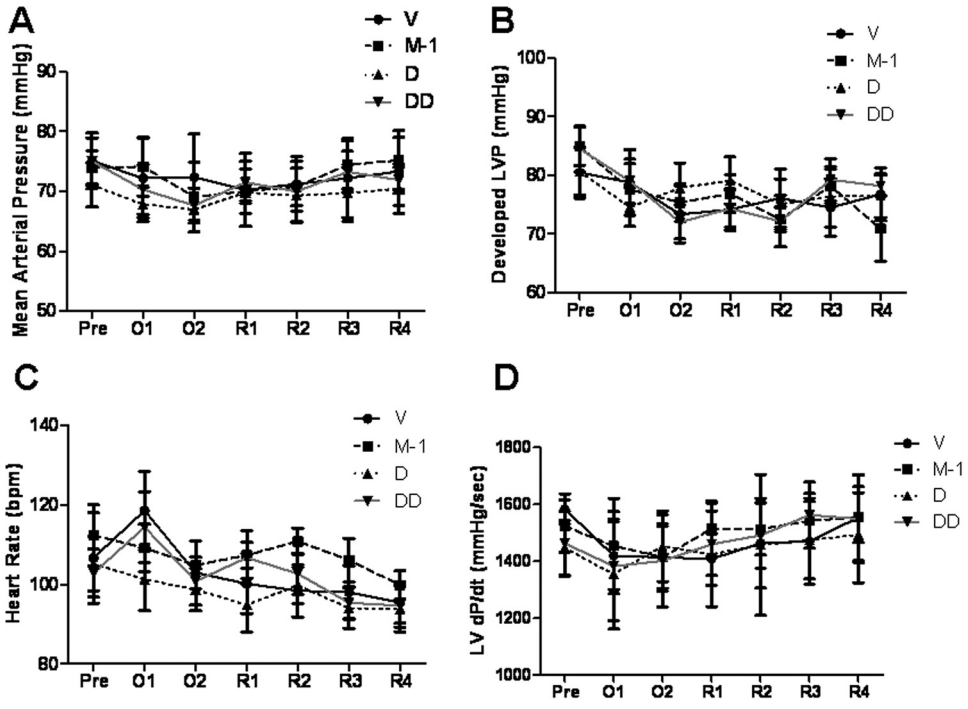

Fig. 3. Global and regional myocardial function. A, MAP. B, developed LVP. C, HR. D, LV systolic function as determined by +LV dP/dt. No significant differences were observed among groups (MAP, $p = 0.93$; HR, $p = 0.61$; LV dP/dt, $p = 0.51$; developed LVP, $p = 0.94$; two-way repeated-measures ANOVA). Pre, preocclusion.

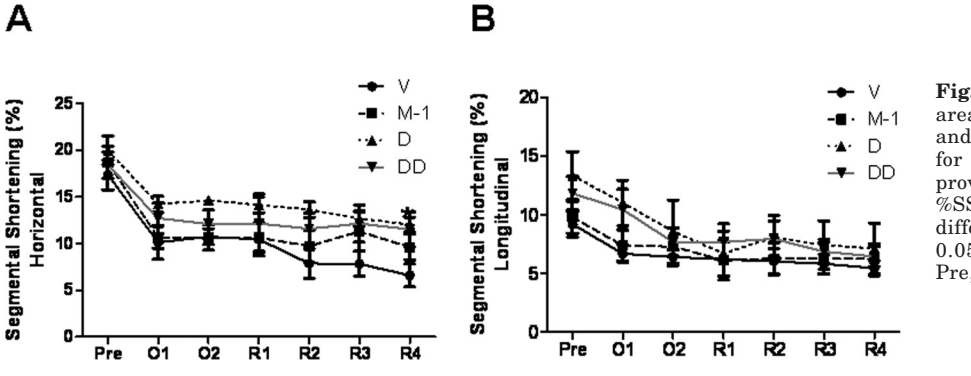

Fig. 4. Regional myocardial function in the area at risk. The %SS in horizontal axes (A) and longitudinal axes (B) is shown. The %SS for the horizontal axis was significantly improved in the D group ($p = 0.04$), whereas the %SS for the longitudinal axis did not show differences among groups ($p = 0.51$). *, $p < 0.05$; two-way repeated-measures ANOVA. Pre, preocclusion.

0.93), HR ($p = 0.61$), LV dP/dt ($p = 0.51$), and developed LVP ($p = 0.94$). Regional myocardial function in the area at risk is shown in Fig. 4. The %SS for horizontal axis was improved in the D group ($p = 0.04$), whereas %SS for longitudinal axis did not show the differences among groups ($p = 0.51$). For M-1/10 and M-4 the data (pre and R4) are shown in Table 2. There are no significant differences compared with vehicle.

Incidence of VF/VT. There was no difference in incidence of VF/VT during ischemia (V, 5/6 animals with VF/VT/total number; M-1, 5/6; D, 4/6; DD, 5/6; χ^2 $p = 0.82$) or reperfusion (V, 0/6; M-1, 1/6; D, 1/6; DD, 0/6; χ^2 $p = 0.90$). As demonstrated previously (Osipov et al., 2009b), VF/VT appeared 15 to 20 min after the beginning of ischemia. All dysrhythmias were successfully terminated with intravenous lidocaine and electrical cardioversion. There was no mortality in the different groups.

Myocardial Infarct Size. The size of the ischemic AAR, expressed as a percentage of total LV mass, was not significantly different among groups (V, 33.7 ± 2.0; M-1, 38.4 ± 3.8; D, 37.1 ± 3.6; DD, 33.7 ± 2.1; $p = 0.59$) (Fig. 5A), whereas the size of the infarct area expressed as a percentage of AAR was decreased in the M-1, D, and DD groups versus V (V, 60.7 ± 9.8; M-1, 41.2 ± 9.6; D, 28.3 ± 2.2; DD, 41.1 ± 8.4; $p < 0.01$) (Fig. 5B).

TABLE 2
Global and regional myocardial function
Values are mean ± S.E., $n = 6$ per group.

	M-1/10 ($n = 6$)	M-4 ($n = 6$)	p
MAP (mm Hg)			
Pre	78.5 ± 4.8	75.5 ± 4.9	NS
R4	66.6 ± 4.6	65.4 ± 5.6	NS
HR (bpm)			
Pre	117.2 ± 8.2	110.3 ± 10.3	NS
R4	102.1 ± 3.6	96.9 ± 6.1	NS
LV dP/dt			
Pre	1651 ± 124	1579 ± 105	NS
R4	1438 ± 132	1412 ± 124	NS
Developed LVP			
Pre	87.1 ± 5.4	82.5 ± 3.9	NS
R4	72.5 ± 4.9	72.9 ± 4.3	NS
%SS (H)			
Pre	17.5 ± 1.8	18.0 ± 2.2	NS
R4	10.6 ± 3.1	11.0 ± 3.2	NS
%SS (L)			
Pre	10.9 ± 1.8	9.2 ± 1.1	NS
R4	7.0 ± 1.3	5.0 ± 0.9	NS

bpm, beat per minute; H, horizontal axis; L, longitudinal axis; Pre, preocclusion. NS, not significant, $P > 0.05$, two-way repeated measures ANOVA.

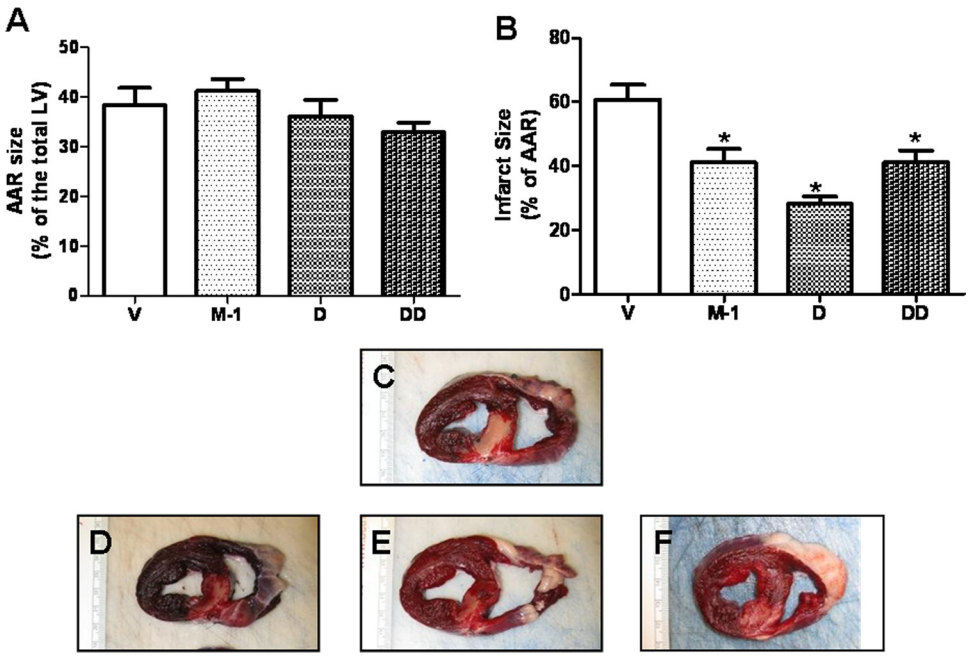

Fig. 5. Myocardial ischemic AAR and infarct size. A, AAR as a percentage of total LV mass ($p = 0.59$). B, infarct size as a percentage of AAR ($p < 0.01$). C–F, representative images of the myocardium after TTC staining are shown in vehicle (C), M group (D), D group (E), and DD group (F). The pictures represent the fourth slices cut into 1-cm-thick slices perpendicular to the axis of the left anterior descending artery after TTC staining. Three zones can be differentiated: nonischemic area (dark red), AAR (bright red), and necrotic area (pale). The size of the infarct area expressed as a percentage of total LV mass was significantly decreased in the M, D, and DD groups versus V ($p < 0.01$; *, $p < 0.05$; one-way ANOVA).

The M-4 group showed a significant decrease in the size of infarct area as a percentage of AAR, whereas the M-1/10 group was almost even with V (M-1/10, 57.3 ± 2.9; M-4, 44.5 ± 3.9). The dose-dependent effect of TP508 monomer and dimer on myocardial protection after AMI-RI is shown in Fig. 6 (M-2 was cited from previous work; M-2 receives twice M-1: $n = 6$) (Osipov et al., 2009b).

Coronary Microvascular Reactivity in the Ischemic Territory. The baseline diameter was 174 ± 12, 143 ± 15, 151 ± 19, and 191 ± 23 μm in groups V, M, D, and DD, respectively ($p = 0.16$). The percentage of precontraction was −33.7 ± 1.9, −34.5 ± 1.7, −32.4 ± 1.7, and −35.3 ± 2.4 in groups V, M, D, and DD, respectively ($p = 0.20$). Receptor-mediated, endothelium-dependent relaxations to ADP were improved in groups D and DD ($p < 0.01$) and endothelium-dependent relaxations to substance P were improved in the M group ($p = 0.03$), whereas endothelium-independent relaxations to SNP were improved in group D ($p = 0.04$) (Fig. 7).

Western Blotting. Expression of phosphorylated (Ser70) Bcl-2 showed significant differences among groups ($p < 0.01$), whereas total Bcl-2 was similar among groups ($p = 0.21$) (Fig. 8, A and B). Expression of total PARP ($p = 0.52$) was not significantly different among groups, whereas cleaved PARP ($p = 0.02$) was significantly lower in groups M, D, and DD compared with V (Fig. 8, C and D). Expression of cleaved caspace-3 ($p = 0.47$) and total caspase-3 ($p = 0.33$) was not significantly different among groups (Fig. 9, A and B). Expression of HSP27 ($p < 0.01$) and αB-crystallin ($p < 0.01$) was significantly higher in the M and D groups compared with V (Fig. 9, C and D).

TUNEL Staining. The apoptotic cell count per 100 mm^2 in the AAR was higher in V compared with the M, D, and DD groups (V, 59 ± 34; M, 13 ± 3; D, 22 ± 3; DD, 23 ± 3; $p < 0.01$) (Fig. 10). As demonstrated previously (Osipov et al., 2009a,b), most apoptotic cells were cardiomyocytes and located mainly near the necrotic area. The nonischemic area was devoid of TUNEL-positive cells.

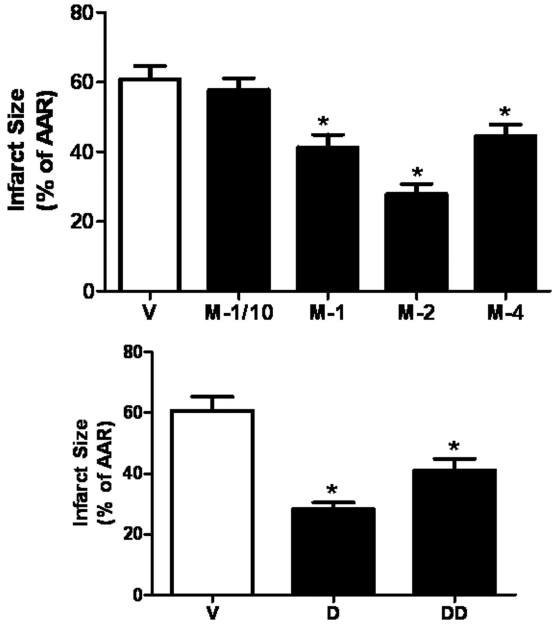

Fig. 6. Dose-dependent effect of TP508 monomer and dimer on the reduction of myocardial infarct area. Myocardial infarct sizes as a percentage of AAR for various TP508 monomer doses (top) and the present dimer series (bottom). M-1/10, M-1, M-2 (M-2 is published data not presented in this study), and M-4 are 0.0216, 0.216, 0.432, and 0.864 μmol/kg as a bolus dose, respectively. M-1, M-2, M-4, D, and DD groups are statistically lower than vehicle ($p < 0.05$). *, $p < 0.05$; one-way ANOVA. In the monomer series, the most effective dose is around M-2, whereas the negative dose response effect can be observed in the dimer series.

Discussion

The most significant finding of this study is that intravenous therapeutic administration of TP508 dimer also has significant myocardial-protective effect in response to AMI-RI as described in previous work with TP508 monomer.

TP508 limited myocardial infarct size, probably via changing protein expression in cell survival/death and apoptosis

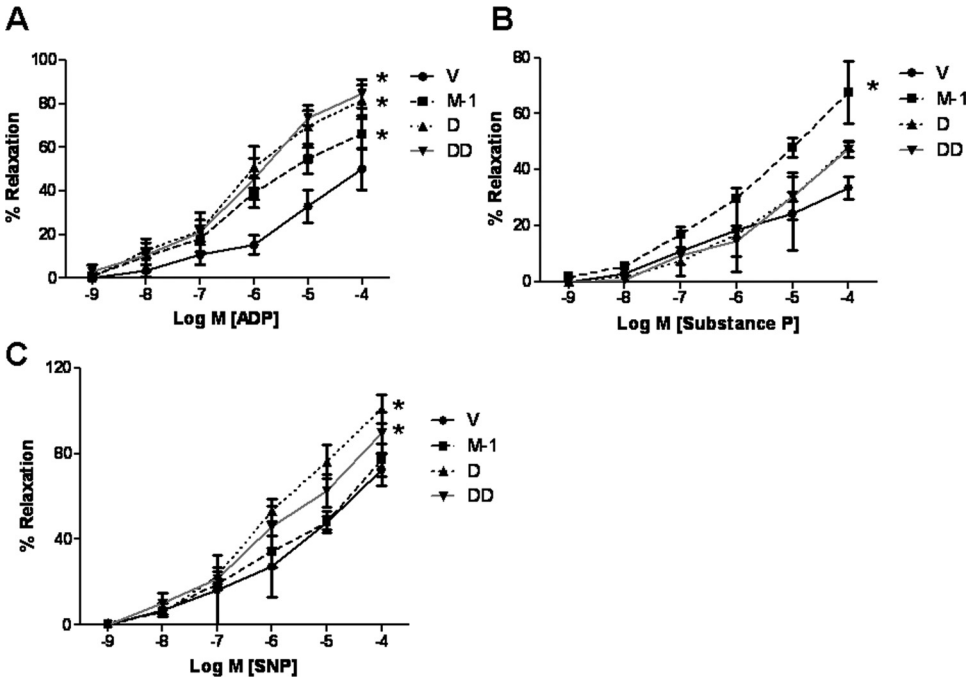

Fig. 7. Coronary microvascular reactivity. A and B, responses are shown to endothelium-dependent agents ADP (A) and substance P (B). C, response to endothelium-independent agent SNP is shown. Responses to ADP were improved in the D and DD groups ($p < 0.01$), response to substance P was improved in the M group ($p = 0.03$), and response to SNP (C) was improved in the D group ($p = 0.04$). *, $p < 0.05$; two-way repeated-measures ANOVA.

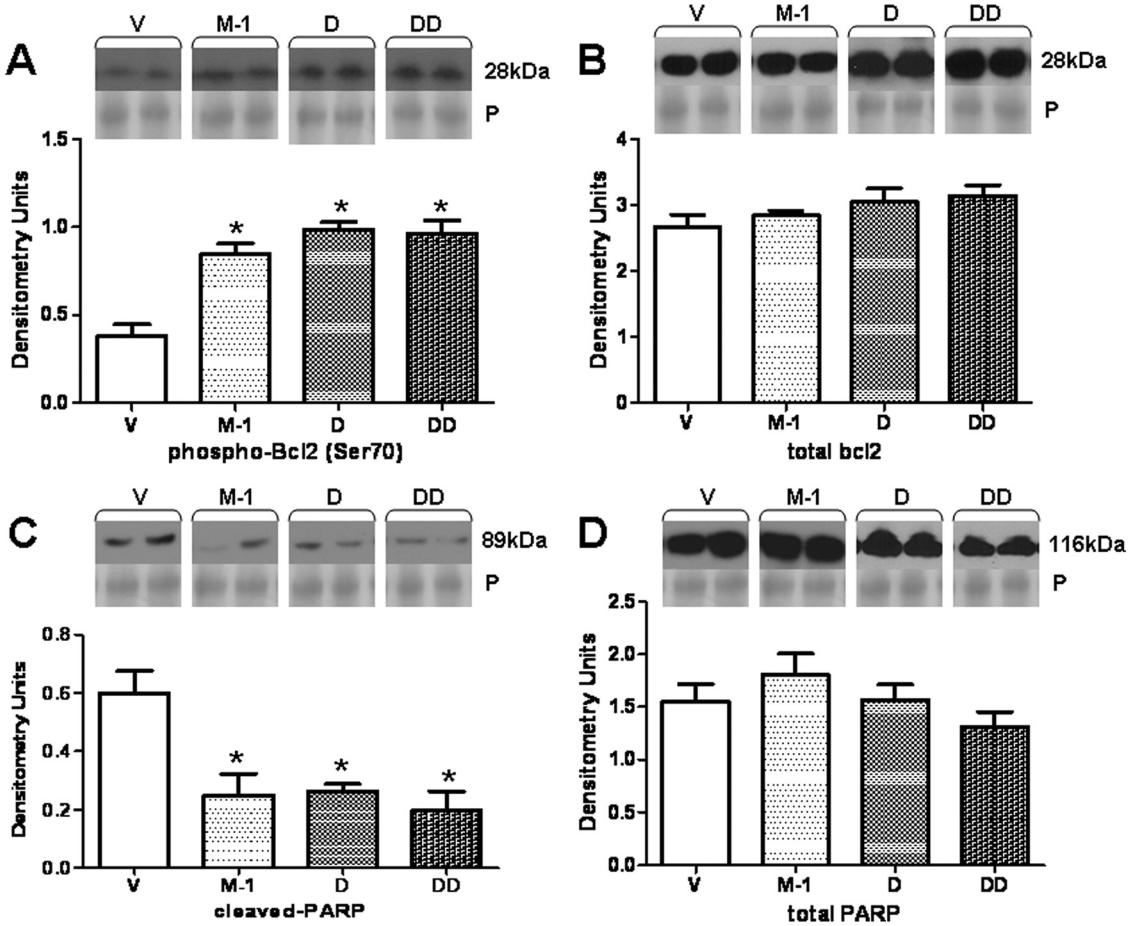

Fig. 8. Protein levels in the AAR. Western blotting of AAR tissue for total and phospho (Ser70) Bcl-2 (A and B) and total and cleaved PARP (C and D) is shown. Representative Western blots and ponceau staining (P) for gels are shown. Values are mean ± S.E.M. in arbitrary densitometry units and compare vehicle ($n = 6$), TP508 monomer group (M-1, $n = 6$), and two doses of dimer groups (D and DD, $n = 6$). *, $p < 0.05$; one-way ANOVA. Phospho Bcl-2 (Ser70) was significantly higher in the M-1, D, and DD groups versus V ($p < 0.01$), whereas total Bcl-2 showed no significant differences among groups ($p = 0.21$). Cleaved PARP ($p = 0.02$) was significantly lower in the M-1, D, and DD groups versus V, whereas total PARP ($p = 0.52$) was not significantly different among groups.

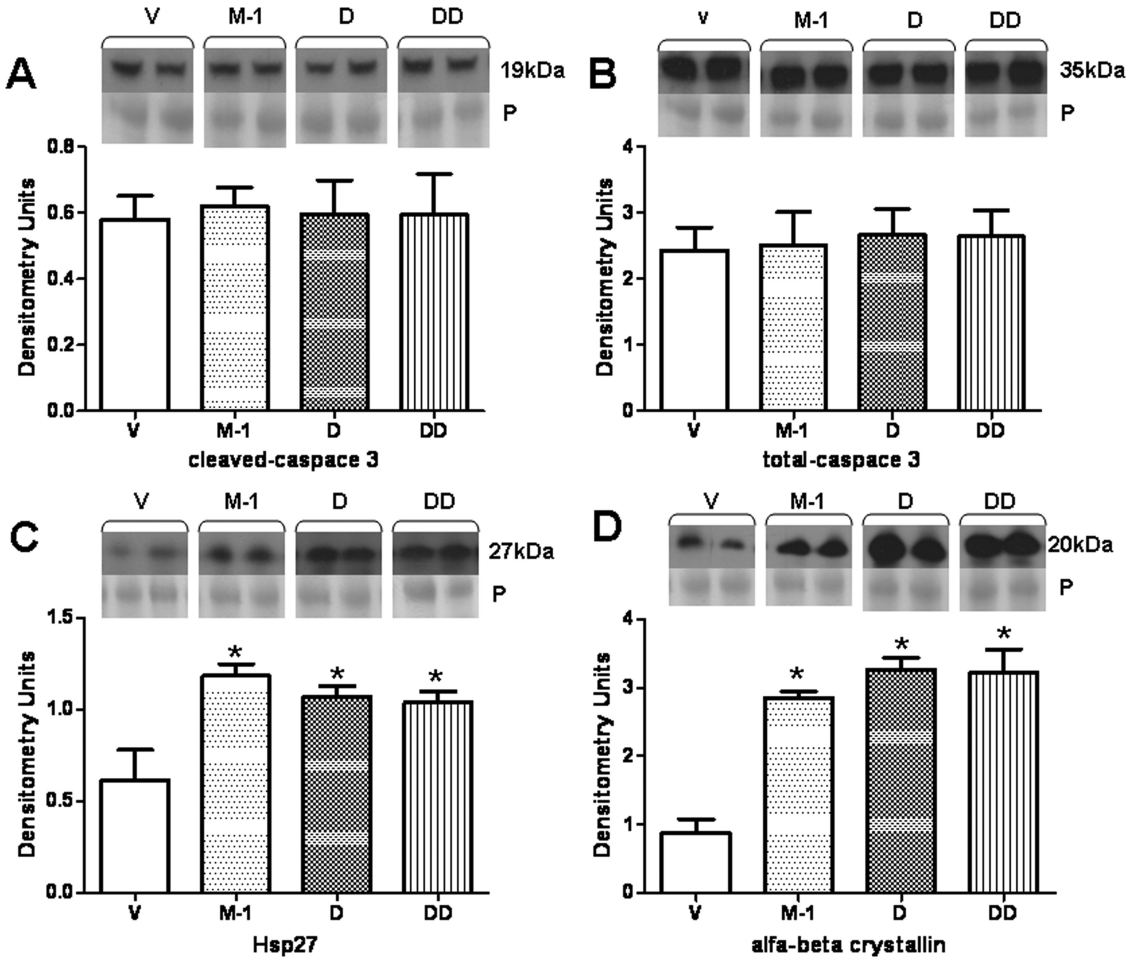

Fig. 9. Protein levels in the AAR. Western blotting of AAR tissue for total and cleaved caspase 3 (A and B), HSP27 (C), and αB-crystallin (D) is shown. HSP27 ($p < 0.01$) and αB-crystallin ($p < 0.01$) showed significantly higher expression in the M-1, D, and DD groups versus V. *, $p < 0.05$; one-way ANOVA.

pathways in a clinically relevant large-animal model. In addition, this study is novel in that we compared the effect of TP508 monomer and dimer in vivo. Administration of two different doses of TP508 dimer in the present study significantly reduced myocardial infarct size compared with vehicle and TP508 monomer. The expression of cleaved PARP was significantly decreased, whereas the expression of phospho Bcl-2 (Ser70), HSP27, and αB-crystalline was significantly increased in groups treated with monomer and two doses of dimer compared with vehicle.

As demonstrated previously, TP508 monomer treatment is associated with higher levels of specific cell survival proteins in the ischemic myocardium, such as heat shock proteins (Osipov et al., 2009b). This study shows that the expression of HSP27 and αB-crystalline was significantly higher in the M-1, D, and DD groups compared with vehicle without any dose-dependent correlation regarding groups receiving two doses of dimer. Recent studies demonstrate that the phosphorylated form of HSP27 is a potent antiapoptotic molecule that might directly interfere with cell death signaling pathways (Benn et al., 2002; Stetler et al., 2009). A number of studies have shown that overexpression of HSP27 reduces apoptotic cell death triggered by various stimuli, including hyperthermia, oxidative stress, staurosporine-induced apoptosis, and cytotoxic drugs (Garrido et al., 1996, 1997; Mehlen et al., 1996; Samali and Cotter, 1996). There is some controversy as to whether HSP27 has direct interaction with caspase-3, although HSP27 has been shown to inhibit apoptosis via the direct inhibition of caspase-3 activation (Garrido et al., 1996, 1999; Concannon et al., 2001; Samali et al., 2001) and through interacting with the pro-caspase-3 molecule (Garrido et al., 1996; Pandey et al., 2000). However, this theory has been challenged by other studies showing little or no direct interaction between HSP27 and caspase-3 (Garrido et al., 1996; Pandey et al., 2000; Paul et al., 2002). This study indicates no significant difference in the expression of the total and cleaved caspase-3 between the treated and untreated groups, whereas expression of HSP27 was significantly higher in all treated groups. This suggests that the higher levels of HSP27 are not associated with the caspase pathway.

αB-crystalline is known as part of the small HSP family (Taylor and Benjamin, 2005; Bagnéris et al., 2009). The strongly cytoprotective function of αB-crystallin and HSP27 might involve binding to specific components of apoptosis (Mao et al., 2004; Arrigo et al., 2007; Stegh et al., 2008) and autophagy (Carra et al., 2008; Bagnéris et al., 2009). This study shows significantly higher expression of αB-crystallin in treated groups compared with vehicle, suggesting that TP508 dimer might have a cytoprotective effect related to the activation of small HSPs such as αB-crystallin and HSP27 and TP508 monomer during AMI-RI (Fig. 11).

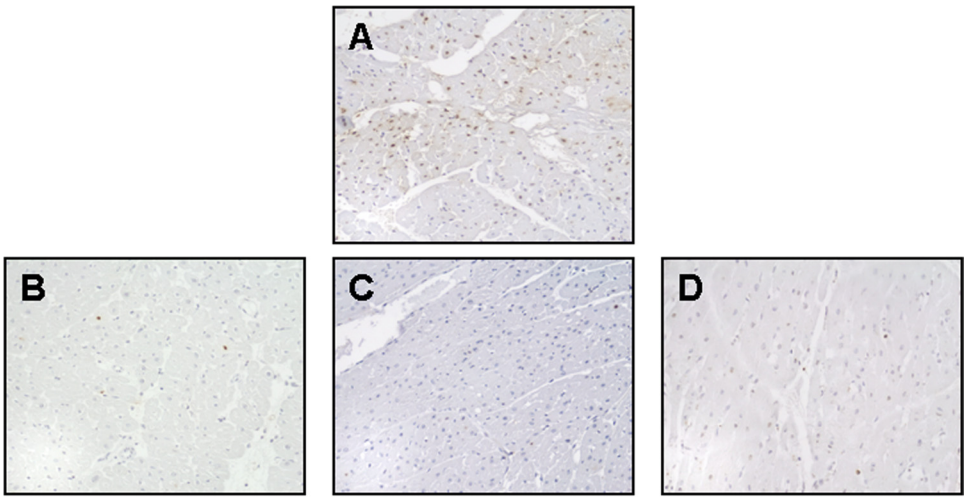

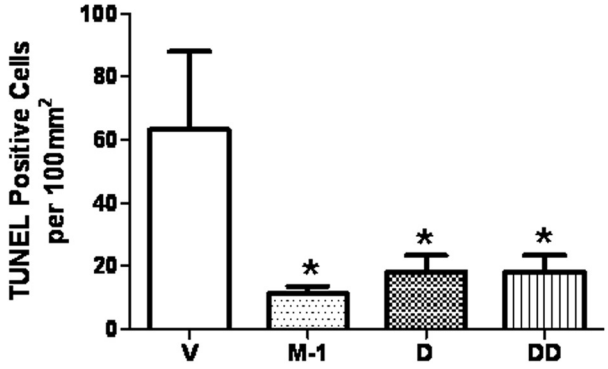

Fig. 10. TUNEL staining. TUNEL-positive cell counts per 100 mm^2 in control (A), M group (B), D group (C), and DD group (D) (four animals per group) are shown. Shown are representative histologic images (×200 magnification). Brown nuclei are the TUNEL-positive cells. M, D, and DD groups versus V, $p < 0.01$. *, $p < 0.01$; one-way ANOVA.

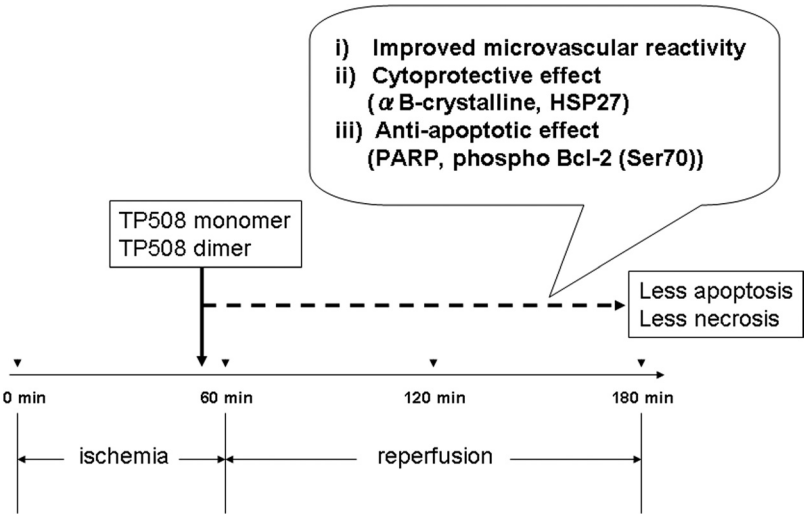

Fig. 11. Summary diagram of TP508 monomer and dimer myocardial-protective properties in the AMI-RI.

PARP is known to help cells maintain their viability, and cleavage of PARP facilitates cellular disassembly and serves as a marker of cells undergoing apoptosis (Osipov et al., 2009b). In this study we found a significant decrease in cleaved PARP in all treated groups compared with vehicle, suggesting that treatment with TP508 monomer and dimer might have an antiapoptotic effect through the cleavage of PARP (Fig. 11). Phosphorylated Bcl-2 (Ser70) is thought to be required for the enhanced antiapototic functions of total Bcl-2 (Deng et al., 2001). This study demonstrates that phospho Bcl-2 (Ser70) was up-regulated in the treated groups, suggesting that TP508 monomer and dimer might have antiapoptotic effects through phosphorylated Bcl-2 (Ser70) (Fig. 11). The TUNEL assay demonstrated that there were fewer apoptotic-positive cells in the TP508-treated groups. Treatment with TP508 monomer and low and high doses of dimer might affect the apoptotic signaling pathway via Bcl-2 and PARP.

The coronary microcirculation, consisting of arterioles less than 175 μm in diameter, is the principal site of resistance in coronary circulation and responds to metabolic stimuli to govern myocardial perfusion (Sodha et al., 2009). Dysfunc-

tion in this vascular bed, which is known to occur after AMI-RI (Hein et al., 2003; Sodha et al., 2009), is thought to be responsible for the impairments in myocardial perfusion observed after re-establishment of flow in the target vessels of thrombolysis, percutaneous coronary intervention, and coronary artery bypass grafting, the large epicardial coronary arteries (Ito et al., 1992). Our previous study suggested that in a hypercholesterolemic swine model TP508 monomer might improve vasodilatation and enhance coronary microvascular relaxation via modulation of nitric oxide signaling (Osipov et al., 2009b). The present study shows improvements in endothelium-dependent vasorelaxation to ADP in coronary microvessels treated with both doses of TP508 dimer. The improved microvascular responses to substance P were seen only in TP508 monomer-treated animals. On the other hand, only the lower dose of the TP508 dimer resulted in improvements in endothelium-independent vasorelaxation to SNP. These results indicate that dimerized TP508 might protect coronary microvasculature against ischemia reperfusion injury. As demonstrated previously, the improvements in coronary microvascular relaxation might have significant clinical relevance. It has been suggested that up to 40% of patients fail to regain appropriate myocardial perfusion despite achieving thrombolysis in myocardial infarction grade 3 epicardial flow after intervention. This might be attributed partly to coronary microvascular dysfunction (Ito et al., 1992; Prasad et al., 2004; Prasad and Gerch, 2005).

Finally, we speculate that the TP508 monomer and dimer exist primarily as their own form based on the in vitro findings, and we suggest that both TP508 monomer and dimer might have dose-dependent effects. It has been reported that the myocardial-protective effect caused by an agent may behave in a dose-dependent manner (Knight et al., 2001; Niemann et al., 2002; Zuo et al., 2009). Our previous study demonstrated TP508 monomer might have a positive effect in a dose-dependent manner within a certain range of administration. In the present study, we performed the additional experiments with administration of very low (1/10 times) and very high (four times) doses of TP508 monomer to verify the dose-dependent response in the more extensive ranges. We found a certain trend of dose-dependent effect on myocardial protection of TP508 monomer (including the published group) (Osipov et al., 2009b) (Fig. 6), suggesting that there is a certain point in which TP508 monomer will be most effective and that excessive dose might not lead to an equivalent benefit. Recent studies demonstrate that hydrogen sulfide (Elrod et al., 2007) and gadolinium (Nicolosi et al., 2008) attenuate AMI-RI dose-dependently and the protective effect might not be increased when associated with increased doses. In this study, the lower dose of TP508 dimer led to a greater reduction in the myocardial infarct size than the higher dose did. This suggests that TP508 dimer, if it is compared with the equivalent dose of TP508 monomer in mole, might provide more protective effect with the lower dose than monomer. It has been suggested that TP508 might be exerting its effects through nonproteolytic interaction with one of the known protease-activated receptors (PAR-1, PAR-3, or PAR-4) or through a separate non-PAR (Coughlin, 2000; Ryaby et al., 2006). It is still unknown whether chemically synthesized TP508 dimer operates with a thrombin-related receptor such as PAR or non-PAR in vivo similarly to TP508 monomer. Further investigation on TP508 dimer will be required to detail the mechanism in vivo.

There are still several limitations in this study. Our time course for tissue harvest (3 h after the onset of ischemia) is not able to account for long-term effects of these drugs on myocardial function and infarct extension and conversely might miss rapid changes in the activation/phosphorylation status of certain apoptotic signaling proteins. In addition, we did not assess the activity levels of these enzymes when we measured the protein concentration of molecules involved with signaling. Finally, the present study does not provide in vivo plasma TP508 data, although we believe that the in vitro data using pig plasma are sufficient to indicate how the monomer and dimer exist in a blood condition. Finally, the present study did not measure the in vivo TP508 monomer and dimer.

In conclusion, therapeutic administration of novel chemically synthesized TP508 dimer before the onset of reperfusion markedly attenuates AMI-RI. This study demonstrates that TP508 dimer also affects apoptotic signaling, limiting apoptosis much like TP508 monomer does. Both TP508 monomer and dimer have a specific dose or range that can provide the most beneficial effect on myocardial protection in the setting of AMI-RI. This study might be a trial worthy of special mention in that dimerization of an existing drug would offer an additional approach for achieving a more stable condition of the drug and finding other beneficial roles for clinical trial.

Acknowledgments

We thank the staff of the Animal Research Facility at the Beth Israel Deaconess Medical Center (Boston, MA) for their efforts.

References

Arrigo AP, Simon S, Gibert B, Kretz-Remy C, Nivon M, Czekalla A, Guillet D, Moulin M, Diaz-Latoud C, and Vicart P (2007) Hsp27 (HspB1) and αB-crystallin (HspB5) as therapeutic targets. *FEBS Lett* **581:**3665–3674.

Bagnéris C, Bateman OA, Naylor CE, Cronin N, Boelens WC, Keep NH, and Slingsby C (2009) Crystal structures of α-crystallin domain dimers of αB-crystallin and Hsp20. *J Mol Biol* **392:**1242–1252.

Benn SC, Perrelet D, Kato AC, Scholz J, Decosterd I, Mannion RJ, Bakowska JC, and Woolf CJ (2002) Hsp27 up-regulation and phosphorylation is required for injured sensory and motor neuron survival. *Neuron* **36:**45–56.

Carney DH, Mann R, Redin WR, Pernia SD, Berry D, Heggers JP, Hayward PG, Robson MC, Christie J, and Annable C (1992) Enhancement of incisional wound healing and neovascularization in normal rats by thrombin and synthetic thrombin receptor-activating peptides. *J Clin Invest* **89:**1469–1477.

Carra S, Seguin SJ, Lambert H, and Landry J (2008) HspB8 chaperone activity toward poly(Q)-containing proteins depends on its association with Bag3, a stimulator of macroautophagy. *J Biol Chem* **283:**1437–1444.

Concannon CG, Orrenius S, and Samali A (2001) Hsp27 inhibits cytochrome *c*-mediated caspase activation by sequestering both pro-caspase-3 and cytochrome *c*. *Gene Expr* **9:**195–201.

Coughlin SR (2000) Thrombin signalling and protease-activated receptors. *Nature* **407:**258–264.

Deng X, Xiao L, Lang W, Gao F, Ruvolo P, and May WS Jr (2001) Novel role for JNK as a stress-activated Bcl2 kinase. *J Biol Chem* **276:**23681–23688.

Elrod JW, Calvert JW, Morrison J, Doeller JE, Kraus DW, Tao L, Jiao X, Scalia R, Kiss L, Szabo C, et al. (2007) Hydrogen sulfide attenuates myocardial ischemia-reperfusion injury by preservation of mitochondrial function. *Proc Natl Acad Sci USA* **104:**15560–15565.

Garrido C, Bruey JM, Fromentin A, Hammann A, Arrigo AP, and Solary E (1999) HSP27 inhibits cytochrome *c*-dependent activation of procaspase-9. *FASEB J* **13:**2061–2070.

Garrido C, Mehlen P, Fromentin A, Hammann A, Assem M, Arrigo AP, and Chauffert B (1996) Inconstant association between 27-kDa heat shock protein (Hsp27) content and doxorubicin resistance in human colon cancer cells. The doxorubicin-protecting effect of Hsp27. *Eur J Biochem* **237:**653–659.

Garrido C, Ottavi P, Fromentin A, Hammann A, Arrigo AP, Chauffert B, and Mehlen P (1997) HSP27 as a mediator of confluence-dependent resistance to cell death induced by anticancer drugs. *Cancer Res* **57:**2661–2667.

Hein TW, Zhang C, Wang W, Chang CI, Thengchaisri N, and Kuo L (2003) Ischemia-reperfusion selectively impairs nitric oxide-mediated dilation in coronary arterioles: counteracting role of arginase. *FASEB J* **17:**2328–2330.

Ito H, Tomooka T, Sakai N, Yu H, Higashino Y, Fujii K, Masuyama T, Kitabatake A,

and Minamino T (1992) Lack of myocardial perfusion immediately after successful thrombolysis. A predictor of poor recovery of left ventricular function in anterior myocardial infarction. *Circulation* **85:**1699–1705.
Knight DR, Smith AH, Flynn DM, MacAndrew JT, Ellery SS, Kong JX, Marala RB, Wester RT, Guzman-Perez A, Hill RJ, et al. (2001) A novel sodium-hydrogen exchanger isoform-1 inhibitor, zoniporide, reduces ischemic myocardial injury in vitro and in vivo. *J Pharmacol Exp Ther* **297:**254–259.
Mao YW, Liu JP, Xiang H, and Li DW (2004) Human αA- and αB-crystallins bind to Bax and Bcl-X(S) to sequester their translocation during staurosporine-induced apoptosis. *Cell Death Differ* **11:**512–526.
Mehlen P, Kretz-Remy C, Préville X, and Arrigo AP (1996) Human hsp27, *Drosophila* hsp27, and human αB-crystallin expression-mediated increase in glutathione is essential for the protective activity of these proteins against TNFα-induced cell death. *EMBO J* **15:**2695–2706.
Nicolosi AC, Strande JL, Hsu A, Fu X, Su J, Gross GJ, and Baker JE (2008) Gadolinium limits myocardial infarction in the rat: dose-response, temporal relations, and mechanisms. *J Mol Cell Cardiol* **44:**345–351.
Niemann CU, Saeed M, Akbari H, Jacobsen W, Benet LZ, Christians U, and Serkova N (2002) Close association between the reduction in myocardial energy metabolism and infarct size: dose-response assessment of cyclosporine. *J Pharmacol Exp Ther* **302:**1123–1128.
Osipov RM, Bianchi C, Clements RT, Feng J, Liu Y, Xu SH, Robich MP, Wagstaff J, and Sellke FW (2009a) Thrombin fragment (TP508) decreases myocardial infarction and apoptosis after ischemia reperfusion injury. *Ann Thorac Surg* **87:**786–793.
Osipov RM, Robich MP, Feng J, Clements RT, Liu Y, Glazer HP, Wagstaff J, Bianchi C, and Sellke FW (2009b) Effect of thrombin fragment (TP508) on myocardial ischemia-reperfusion injury in hypercholesterolemic pigs. *J Appl Physiol* **106:**1993–2001.
Pandey P, Farber R, Nakazawa A, Kumar S, Bharti A, Nalin C, Weichselbaum R, Kufe D, and Kharbanda S (2000) Hsp27 functions as a negative regulator of cytochrome *c*-dependent activation of procaspase-3. *Oncogene* **19:**1975–1981.
Paul C, Manero F, Gonin S, Kretz-Remy C, Virot S, and Arrigo AP (2002) Hsp27 as a negative regulator of cytochrome *c* release. *Mol Cell Biol* **22:**816–834.
Prasad A, Stone GW, Aymong E, Zimetbaum PJ, McLaughlin M, Mehran R, Garcia E, Tcheng JE, Cox DA, Grines CL, et al. (2004) Impact of ST-segment resolution after primary angioplasty on outcomes after myocardial infarction in elderly patients: an analysis from the CADILLAC trial. *Am Heart J* **147:**669–675.
Prasad A and Gersh BJ (2005) Management of microvascular dysfunction and reperfusion injury. *Heart* **91:**1530–1532.
Ryaby JT, Sheller MR, Levine BP, Bramlet DG, Ladd AL, and Carney DH (2006) Thrombin peptide TP508 stimulates cellular events leading to angiogenesis, revascularization, and repair of dermal and musculoskeletal tissues. *J Bone Joint Surg Am* **88:**132–139.
Samali A and Cotter TG (1996) Heat shock proteins increase resistance to apoptosis. *Exp Cell Res* **223:**163–170.
Samali A, Robertson JD, Peterson E, Manero F, van Zeijl L, Paul C, Cotgreave IA, Arrigo AP, and Orrenius S (2001) Hsp27 protects mitochondria of thermotolerant cells against apoptotic stimuli. *Cell Stress Chaperones* **6:**49–58.
Sheller MR, Crowther RS, Kinney JH, Yang J, Di Jorio S, Breunig T, Carney DH, and Ryaby JT (2004) Repair of rabbit segmental defects with the thrombin peptide, TP508. *J Orthop Res* **22:**1094–1099.
Sodha NR, Clements RT, Feng J, Liu Y, Bianchi C, Horvath EM, Szabo C, Stahl GL, and Sellke FW (2009) Hydrogen sulfide therapy attenuates the inflammatory response in a porcine model of myocardial ischemia/reperfusion injury. *J Thorac Cardiovasc Surg* **138:**977–984.
Spurlock ME and Gabler NK (2008) The development of porcine models of obesity and the metabolic syndrome. *J Nutr* **138:**397–402.
Stegh AH, Kesari S, Mahoney JE, Jenq HT, Forloney KL, Protopopov A, Louis DN, Chin L, and DePinho RA (2008) Bcl2L12-mediated inhibition of effector caspase-3 and caspase-7 via distinct mechanisms in glioblastoma. *Proc Natl Acad Sci USA* **105:**10703–10708.
Stetler RA, Gao Y, Signore AP, Cao G, and Chen J (2009) HSP27: mechanisms of cellular protection against neuronal injury. *Curr Mol Med* **9:**863–872.
Stiernberg J, Norfleet AM, Redin WR, Warner WS, Fritz RR, and Carney DH (2000) Acceleration of full-thickness wound healing in normal rats by the synthetic thrombin peptide, TP508. *Wound Repair Regen* **8:**204–215.
Taylor RP and Benjamin IJ (2005) Small heat shock proteins: a new classification scheme in mammals. *J Mol Cell Cardiol* **38:**433–444.
Wang H, Li X, Tomin E, Doty SB, Lane JM, Carney DH, and Ryaby JT (2005) Thrombin peptide (TP508) promotes fracture repair by up-regulating inflammatory mediators, early growth factors, and increasing angiogenesis. *J Orthop Res* **23:**671–679.
Zuo L, Chen YR, Reyes LA, Lee HL, Chen CL, Villamena FA, and Zweier JL (2009) The radical trap 5,5-dimethyl-1-pyrroline *N*-oxide exerts dose-dependent protection against myocardial ischemia-reperfusion injury through preservation of mitochondrial electron transport. *J Pharmacol Exp Ther* **329:**515–523.

Address correspondence to: Dr. Frank W. Sellke, Department of Surgery/Division of Cardiothoracic Surgery, Rhode Island Hospital and Alpert Medical School, Brown University, 592 Eddy Street, APC 424, Providence, RI 02903. E-mail: fsellke@lifespan.org